Yasuyuki Yamashita, MD • Miyuki Torashima, MD • Mutsumasa Takahashi, MD • Nobuyuki Tanaka, MD
Hidetaka Katabuchi, MD • Kohji Miyazaki, MD • Masaharu Ito, MD • Hitoshi Okamura, MD

Hyperintense Uterine Leiomyoma at T2-weighted MR Imaging: Differentiation with Dynamic Enhanced MR Imaging and Clinical Implications[1]

PURPOSE: **To evaluate the role of dynamic enhanced magnetic resonance (MR) imaging in differentiating leiomyomas with high signal intensity at T2-weighted imaging.**

MATERIALS AND METHODS: **Histologic features of 34 uterine leiomyomas that showed hyperintensity on T2-weighted images were compared with those of ordinary hypointense leiomyomas (n = 74). The results of treatment with gonadotropin-releasing hormone analogue were also analyzed in relation to pretreatment signal intensity.**

RESULTS: **Degenerated leiomyomas (n = 13) had higher signal intensity and heterogeneous architecture, but there was considerable overlap in signal intensity with cellular leiomyomas (n = 21). At dynamic enhanced MR imaging, cellular leiomyomas had marked contrast enhancement in the early phase, while degenerated leiomyomas showed slight or irregular enhancement. Cellular leiomyomas were reduced significantly in size after treatment (P = .02). The response in degenerated leiomyomas was minimal.**

CONCLUSION: **Evaluation of signal intensity at T2-weighted imaging and degree of contrast enhancement at dynamic enhanced MR imaging provide useful information on the nature of leiomyomas.**

Index terms: Hormones • Myoma, 854.318 • Uterine neoplasms, diagnosis, 854.12143, 854.318

Radiology 1993; 189:721–725

ALTHOUGH leiomyomas have been known to show various signal intensities on T2-weighted magnetic resonance (MR) images, most uterine leiomyomas appear as sharply marginated, homogeneous focal areas of decreased signal intensity due to the T1 and T2 relaxation times of smooth muscle (1). On the other hand, degenerated leiomyomas demonstrate inhomogeneous signal intensity, with degenerated regions displaying higher signal intensity than nondegenerated regions (2). A leiomyoma with a higher degree of cellularity also shows higher intensity than that of the myometrium (3).

In patients who wish to preserve fertility, medical treatment with gonadotropin-releasing hormone (Gn-RH) analogues is considered an alternative to hysterectomy. Not only total uterine volume but also the individual volume of the leiomyoma can be quantitatively assessed with MR imaging (4,5). However, the effectiveness of Gn-RH analogues in reducing the size of leiomyomas is variable, and adverse effects such as the development of osteoporosis may occur (6). Consequently, it would be beneficial if we could predict the effect of medical treatment by use of MR imaging.

In this study, we analyzed histologic findings in leiomyomas that showed hyperintensity at T2-weighted MR imaging and evaluated the role of dynamic gadolinium-enhanced MR imaging. We also analyzed the results of treatment with Gn-RH analogues in relation to T2-weighted and dynamic MR appearances.

MATERIALS AND METHODS

This study was composed of two parts: (*a*) correlation between preoperative MR imaging results and hysterectomy specimens and (*b*) evaluation of the effect of medical treatment as predicted with pretreatment MR imaging.

Pathologic-Radiologic Correlation in Excised Leiomyomas

The study population consisted of 83 women (108 leiomyomas) who underwent myomectomy or hysterectomy between January 1990 and December 1992. The diameter of the leiomyomas ranged from 3 to 21 cm; 70 were intramural, 28 were subserosal, six were submucosal, two were cervical, one was located in the broad ligament, and one was located in the isthmus. Conventional T1- and T2-weighted spin-echo (SE) studies were performed in all patients, and 34 hyperintense leiomyomas (signal intensity of leiomyoma higher than that of myometrium on T2-weighted SE images) were identified (size range, 3–17 cm; 19 were subserosal, 14 were intramural, and one was in the isthmus). Dynamic enhanced MR imaging was performed in 27 patients with hyperintense leiomyomas. In 15 patients with hypointense leiomyoma who had concomitant diseases (multiple leiomyomas of various signal intensities, endometrial cancer, etc), dynamic enhanced MR imaging of the leiomyomas was also performed. Patients who received hormone therapy were not included in this study group.

Histologic sections of leiomyoma from all patients, stained with hematoxylin-eosin, were reviewed by a gynecologic pathologist (H.K.) who was unaware of the MR findings. In patients with more than one tumor, each tumor was evaluated separately. All MR and pathologic findings were analyzed separately and then correlated with reference to macroscopic findings in order to correspond to the specific tumor seen at MR imaging.

Evaluation of Treatment Effect with Pretreatment MR Imaging in Medical Treatment Group

Twenty-seven women aged 35–56 years (mean, 46.1 years) with 38 uterine leiomyomas were treated with Gn-RH analogue (buserelin; Suprecur, Hoechst Japan Pharmaceuticals, Tokyo, Japan). Starting

Abbreviations: Gn-RH = gonadotropin-releasing hormone, SE = spin echo.

[1] From the Departments of Radiology (Y.Y., M. Torashima, M. Takahashi) and Gynecology and Obstetrics (N.T., H.K., K.M., M.I., H.O.), Kumamoto University School of Medicine, 1-1-1 Honjo, Kumamoto 860, Japan. Received March 29, 1993; revision requested May 6; revision received July 19; accepted July 30. **Address reprint requests to** Y.Y.

on day 2 of their menstrual cycles, the analogue was self-administered by means of intranasal insufflation of 300 μg for 6 months. T1- and T2-weighed SE images were obtained in all patients, and dynamic enhanced MR imaging was performed in patients with hyperintense leiomyomas. Leiomyomas treated with Gn-RH analogue were categorized into three types depending on the pretreatment T2-weighted and dynamic enhanced MR findings (see "Results" section), and results were correlated with results of treatment.

MR Imaging Examination and MR Image Analysis

MR imaging was performed with a 1.5-T superconductive unit (Magnetom; Siemens Medical Systems, Erlangen, Germany). T1-weighted SE images were obtained with a repetition time (TR) of 600 msec, an echo time (TE) of 15 msec (TR/TE = 600/15), a 256 × 192 matrix, and two excitations. T2-weighted SE images were obtained with a TR of 2,000 msec, a TE of 70 msec, a 256 × 256 matrix, and one excitation.

Dynamic MR images were obtained immediately and then every 30 seconds for 3 minutes after rapid injection (2 mL/sec) of gadopentetate dimeglumine (Magnevist; Japan Schering, Osaka, Japan) (0.1 mmol/kg of body weight) by using an SE technique with a TR of 200 msec, a TE of 15 msec, a 256 × 128 rectangular matrix, and one excitation. Actual sampling time per image was 25.6 seconds. Postcontrast T1-weighted images were obtained 5–6 minutes after injection of gadopentetate dimeglumine. Both conventional SE and dynamic enhanced images were obtained with a section thickness of 7 mm and a 2-mm gap.

For surgical patients, multiple regions of interest of 4–10 mm^2 were selected in the predominant area of signal intensity in the leiomyoma and myometrium, and the average values were obtained. The contrast-to-noise ratio between the leiomyoma and the myometrium was obtained as follows: $(S_l - S_m)$/noise SD, where S_l indicates the signal intensity of the leiomyoma, S_m the signal intensity of the myometrium, and noise SD the standard deviation of the intensity of the background noise in the phase-encoding direction. The Student *t* test was employed to determine the significance of the difference in contrast-to-noise ratio between the pulse sequences.

Patients who received Gn-RH therapy underwent MR imaging and ultrasound (US) before receiving treatment and were followed up every 2 months with either US or MR imaging. The treatment effects were evaluated at 6 months (the completion of treatment) with MR imaging. The leiomyoma volume was calculated by means of the formula for the volume of an ellipse (length × width × depth × π/6), and the ratio of the volume before and after treatment for each tumor was calculated. The change in tumor volume after treatment was analyzed with the Wilcoxon test. Comparison of treatment effect in each group was done with the Tukey Studentized range test.

All MR images, including both conventional SE and dynamic enhanced images in both the surgically and medically treated groups, were interpreted blindly by two investigators (Y.Y., M. Torashima) without knowledge of pathologic results or treatment status. Initially, images were interpreted independently, and consensus was obtained in conference.

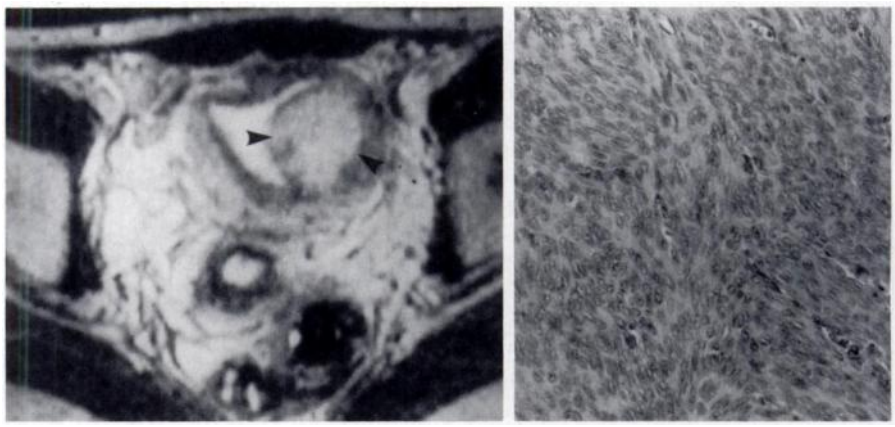

Figure 1. Images of cellular submucosal leiomyoma in a 32-year-old woman. **(a)** T2-weighted SE image (2,000/70) reveals a relatively homogeneous tumor with high signal intensity compared with that of myometrium in the left side of the uterine corpus (arrowheads). **(b)** Photomicrograph shows the tumor to be composed of densely packed cellular fascicles of smooth muscle with little intervening collagen. No degenerative changes are seen. (Hematoxylin-eosin stain; original magnification, ×100.)

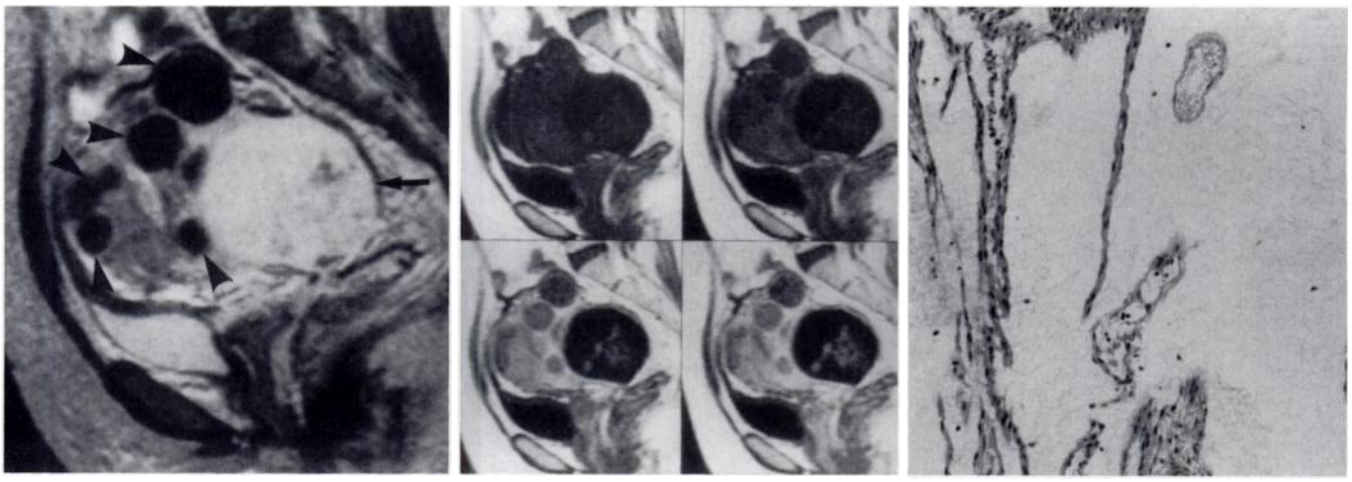

Figure 2. Images of multiple leiomyoma in a 61-year-old woman. **(a)** T2-weighted SE image (2,000/70) reveals multiple leiomyomas in the uterus. Most leiomyomas are hypointense (arrowheads), but the largest leiomyoma in the posterior wall is hyperintense (arrow) compared with the myometrium. **(b)** Dynamic enhanced images (200/15) obtained after administration of gadopentetate dimeglumine show slight enhancement of hypointense leiomyomas. In the largest, hyperintense leiomyoma, enhancement is seen only in the central area, suggesting that most areas of the tumor are degenerated. **(c)** Representative photomicrograph of hyperintense leiomyoma demonstrates severe hyaline and mucinous degeneration and ordinary myoma cells. (Hematoxylin-eosin stain; original magnification, ×100.)

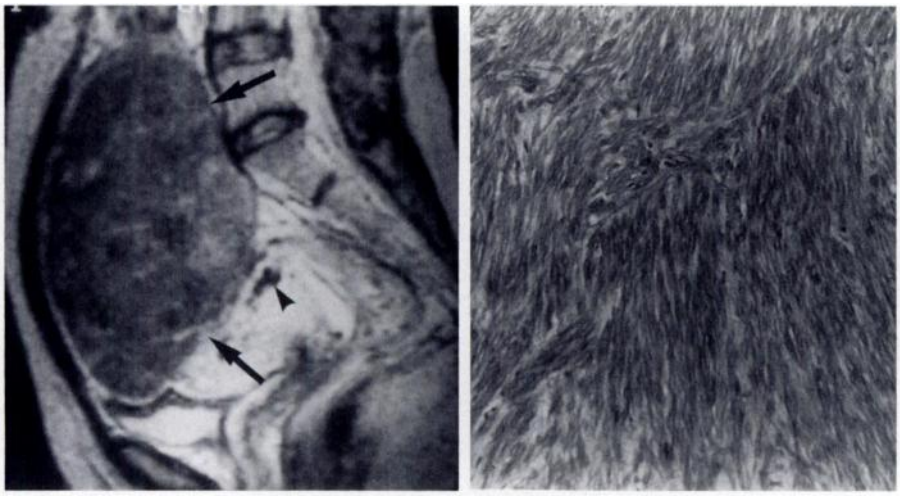

a. b.

Figure 3. Images of ordinary hypointense subserous leiomyoma in a 38-year-old woman. **(a)** T2-weighted SE image (2,000/70) reveals a large tumor that is predominantly hypointense (arrows) compared with the myometrium. Tortuous vessels (arrowhead) are seen around the tumor. **(b)** Representative photomicrograph of the leiomyoma shows typical whorls of smooth muscle cells with intervening collagen. No degenerative changes are seen. (Hematoxylin-eosin stain; original magnification, ×100.)

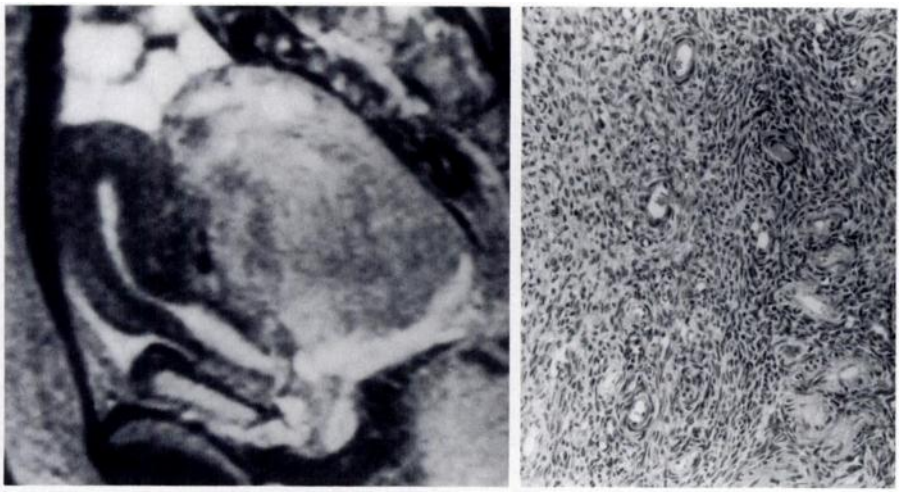

a. b.

Figure 4. Images of cellular leiomyoma mimicking a solid ovarian tumor in a 38-year-old woman. **(a)** T2-weighted SE image (2,000/70) reveals a relatively homogeneous tumor with high signal intensity compared with that of myometrium in the cul-de-sac. Preoperative diagnosis was a left ovarian tumor, probably malignant. **(b)** Photomicrograph shows the tumor to be composed of bizarre leiomyoma cells, which originated from the left isthmus. (Hematoxylin-eosin stain; original magnification, ×100.)

Table 1
Contrast-to-Noise Ratios and Patterns of Enhancement of Leiomyomas

	Histologic Subtype of Leiomyoma		
	Cellular (n = 21)	Degenerated (n = 13)	Ordinary (n = 74)
Contrast-to-noise ratio			
Mean value	4.7*	9.1*	−4.4
95% confidence interval	1.9 to 7.4	4.3 to 13.8	−7.1 to −1.7
Pattern of enhancement†			
Homogeneous	17	0	3
Irregular	1	2	5
Peripheral or minimal	0	8	7

* No significant difference with Student t test.
† Pattern of enhancement was evaluated with dynamic enhanced study. Numbers of patients (n = 18 for cellular leiomyomas, n = 10 for degenerated leiomyomas, and n = 15 for ordinary leiomyomas).

RESULTS

Radiologic-Pathologic Correlation

By evaluating macroscopic findings and pathologic slides, hyperintense leiomyomas were categorized as either (*a*) cellular leiomyoma (n = 21), predominantly composed of densely packed cellular fascicles of smooth muscle with little intervening collagen (Fig 1), or (*b*) degenerated leiomyoma (n = 13), composed of ordinary leiomyoma cells with extensive degenerative changes (hyalin degeneration, myxomatous degeneration, hemorrhage, cystic change, fatty change, etc) (Fig 2). Hypointense leiomyomas (n = 74) were predominantly composed of typical whorls of smooth muscle cells, although degeneration and cellular components were partially seen (termed "ordinary leiomyoma") (Fig 3). There was no significant difference in size and location between these three types. Among cellular leiomyomas, two tumors were diagnosed as atypical leiomyoma (bizarre leiomyoma) (Fig 4) and one as borderline malignancy because of cytologic atypia with higher mitosis of tumor cells (7).

Although degenerated leiomyomas tended to have higher signal intensity than cellular leiomyomas, there was considerable overlap in signal intensity (no significant difference, Table 1). Cellular leiomyomas were usually homogeneous (16 of 21 tumors), while degenerated leiomyomas were markedly heterogeneous, with mixed hypo- and hyperintense signal in eight of 13 tumors. However, it appeared to be difficult to differentiate between these two types with conventional T2-weighted imaging. In contrast to degenerated and cellular leiomyomas, ordinary leiomyomas were very hypointense, with only minimally increased signal intensity compared with that of myometrium (Fig 3).

Dynamic enhanced MR imaging was performed in 18 cellular leiomyomas, 10 degenerated leiomyomas, and 15 ordinary leiomyomas. Most cellular leiomyomas showed remarkable and homogeneous contrast enhancement in the early dynamic phase (30–90 seconds after administration of gadopentetate dimeglumine) (Fig 5). Degenerated leiomyomas showed irregular, peripheral, or minimal enhancement compared with that of myometrium, depending on the degeneration within the tumor (Fig 2). Ordinary leiomyoma showed irregular, peripheral, or minimal enhancement (Fig 2). Cellular and degenerated leiomyomas

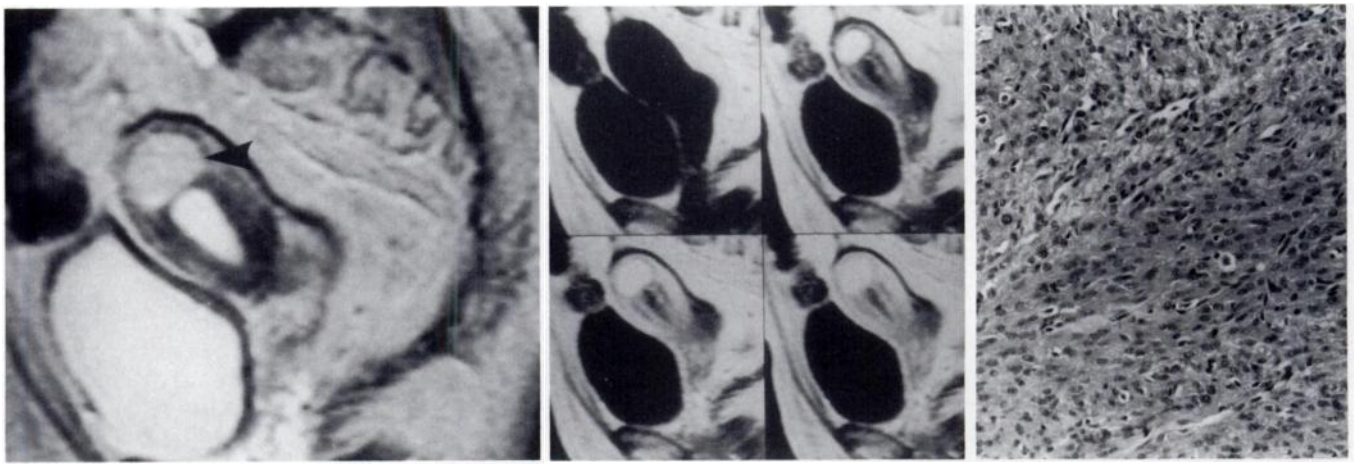

a. b. c.

Figure 5. Images of cellular leiomyoma in a 45-year-old woman. **(a)** T2-weighted SE image (2,000/70) reveals a homogeneous tumor with high signal intensity (arrowhead) in comparison with that of the myometrium. **(b)** Dynamic enhanced images (200/15) obtained after administration of gadopentetate dimeglumine show homogeneous marked contrast enhancement of the tumor. **(c)** Photomicrograph shows the tumor to be composed of densely packed cellular fascicles of smooth muscle with little intervening collagen. No degenerative changes are seen. (Hematoxylin-eosin stain; original magnification, ×100.)

were correctly differentiated in most cases on the basis of enhancement pattern (Table 1).

Response to Medical Treatment in Relation to MR Appearance

Of the 38 leiomyomas treated with Gn-RH analogues, 10 tumors that showed homogeneous hyperintensity with considerable enhancement were considered cellular leiomyoma. Six heterogeneously hyperintense tumors with slight or irregular enhancement were regarded as degenerated leiomyoma. The other 22 tumors were considered ordinary hypointense leiomyoma.

In cellular leiomyomas, tumor volume was reduced significantly after treatment ($P = .02$), while there was no significant reduction in the volume of degenerated leiomyomas (Table 2). The response in ordinary leiomyomas was variable but not statistically significant. There was a significant difference in response to treatment between cellular leiomyomas and degenerated leiomyomas ($P < .01$). The signal intensity did not change in ordinary and degenerated leiomyomas after treatment. Among cellular leiomyomas, six remained hyperintense and four became hypointense.

DISCUSSION

Ordinary leiomyomas are characterized by whorled bundles of smooth muscle cells separated by a greater or lesser amount of vascularized connective tissue. Foci of fibrosis, hyalin degeneration, fatty metamorphosis, calcification, and ischemic necrosis with hemorrhage may occur in various degrees. The term *degenerated leiomyoma* is used for tumors with predominant degenerative characteristics. Cellular leiomyoma is a specific subtype of leiomyoma composed of densely packed cellular fascicles of smooth muscle with little intervening collagen. The cytoplasm is usually abundant. Tumors having bizarre tumor cells with variation in size and shape, hyperchromatic nuclei, and multinucleated form, but no increased mitotic activity, are designated bizarre leiomyoma (Fig 4). Leiomyomas composed of cellular fascicles with greater mitotic activity may be leiomyosarcoma (7). One might expect that uterine leiomyosarcomas would have higher signal intensity and be less well defined than leiomyomas, but thus far there has not been sufficient experience with MR imaging in differential diagnosis of these rare malignancies (8). This differentiation can be done only histologically (7).

The signal intensity of leiomyoma varies depending on degeneration or cellular content (1–3). Differentiation between hyaline, myxomatous, fatty, or mucinous degeneration and hypercellularity or malignant transformation has not been possible at MR imaging (1). In our study, slightly hyperintense tumors were more likely to be cellular leiomyoma, while markedly hyperintense tumors with heterogeneous architecture tended to be degenerated. However, there seemed to be considerable overlap in MR appearance between these two types on conventional T2-weighted images. Cellular or degenerated subserosal leiomyomas also need to be differentiated from ovarian or other pelvic tumors (Fig 4).

Table 2
Leiomyoma Volume before and after Treatment

Type of Leiomyoma	Leiomyoma Volume (cm^3)	
	Pre-treatment	Post-treatment
Cellular	322 ± 584*	79 ± 140*
Degenerated	274 ± 302†	228 ± 186†
Ordinary	229 ± 714†	164 ± 289†

Note.—Values are mean ± standard deviation.

* Significant reduction in tumor size with Wilcoxon test.

† No significant reduction compared with pretreatment volume. A significant difference in response to treatment was seen between cellular leiomyoma and degenerated leiomyoma with the Tukey Studentized range test ($P < .01$).

Although contrast enhancement usually does not improve detection or characterization of leiomyomas (9), differentiation of hyperintense leiomyomas could be made with greater specificity. Cellular leiomyomas showed homogeneous contrast enhancement in the early dynamic phase in our study, while degenerated leiomyomas showed minimal or irregular enhancement (Figs 2, 5). Because cellular leiomyomas enhanced prominently in the early dynamic phase, the contrast between the myometrium and the leiomyoma on dynamic enhanced images was superior to that on postcontrast T1-weighted images.

MR imaging can be used to document the regression of leiomyomas

after treatment with Gn-RH analogues (4,5). Successful treatment is depicted as decreased tumor volume and decreased conspicuity of peripheral vessels. Although treatment with Gn-RH analogues results in a decrease in size of the uterine leiomyoma, the development of osteoporosis due to estrogen deprivation can occur (6). Therefore, if we could predict treatment effect before administration of the drug, the potential adverse effects might be avoided.

The mechanism for reduction of leiomyoma after treatment with Gn-RH analogues is not known. It has been shown histologically that leiomyomas treated with Gn-RH analogues reveal significant reduction in cellularity and an increase in hyalin degeneration (10,11). The lack of estrogen caused by administration of Gn-RH analogues may be one of the primary causes of the significant reduction in cellularity and tumor size (10). The response to treatment in hyperintense leiomyomas with contrast enhancement—indicating cellular leiomyoma—was significant, probably because the cellular component is abundant and fibrous tissue is scarce in this type of leiomyoma. In some ordinary leiomyomas with a small amount of fibrous tissue, Gn-RH analogue therapy may be effective. However, this treatment may not be indicated in degenerated leiomyoma. Although cellular and degenerated leiomyomas have similar appearances on conventional T2-weighted images, differentiation between these two varieties can be accomplished with contrast-enhanced MR imaging. Because the number of patients with each type of leiomyoma was limited in this study, further correlation between type of leiomyoma and treatment effect will be required to establish the indication for this treatment.

In conclusion, both degenerated and cellular leiomyomas exhibit hyperintensity at SE MR imaging, but response to treatment with Gn-RH analogues differs significantly between these varieties. Dynamic enhanced MR imaging enables differentiation between these types of leiomyoma. Evaluation of signal intensity with T2-weighted imaging and the pattern of enhancement provide useful information on the nature of leiomyomas and may be helpful in the planning of treatment. ■

ADDENDUM

We recently encountered two cases of hyperintense leiomyoma that were neither cellular nor degenerative. On T2-weighted images, both tumors were irregularly hyperintense, with mixed hyperintense and hypointense areas. On dynamic enhanced MR images, marked enhancement corresponding to hyperintense areas on T2-weighted images was seen. At histologic examination, extensive edema was seen in the interstitial space. Thus, in differentiating hyperintense leiomyomas, the diagnosis of leiomyoma with edema should be considered in addition to the diagnoses of cellular or degenerative leiomyoma.

Acknowledgment: We thank Jungo Sawa, BS, for statistical analysis.

References

1. Hricak H, Tscholakoff D, Heinrichs L, et al. Uterine leiomyoma: correlation of MR, histopathologic findings, and symptoms. Radiology 1986; 158:385–391.
2. Hamlin DJ, Pettersson H, Fitzsimmons J, Morgan LS. MR imaging of uterine leiomyoma and their complications. J Comput Assist Tomogr 1985; 9:902–907.
3. Lee JKT, Gersell DJ, Balfe DM, Worthington JL, Picus D, Gapp G. The uterus: in vitro MR-anatomic correlation of normal and abnormal specimen. Radiology 1985; 157:175–179.
4. Zawin M, McCarthy S, Scoutt L, et al. Monitoring therapy with a gonadotropin-releasing hormone analog: utility of MR imaging. Radiology 1990; 175:503–506.
5. Andreyko JL, Blumenfeld Z, Marshall LA, Monroe SE, Hricak H, Jaffe RB. Use of an agonistic analog of gonadotropin-releasing hormone (nafarelin) to treat leiomyomas: assessment by magnetic resonance imaging. Am J Obstet Gynecol 1988; 158:903–910.
6. Ito M, Sakoda Y, Okamura H. Calcium metabolism in premenopausal women treated by Gn-RH agonist for uterine myoma. Endocrinol Japon 1990; 37:907–913.
7. Zaloudek C, Norris HJ. Mesenchymal tumors of the uterus. In: Kurman RJ, ed. Blaustein's pathology of the female genital tract. 3rd ed. New York, NY: Springer-Verlag, 1987; 373–408.
8. Mitchell DG. Benign disease of the uterus and ovaries: application of magnetic resonance imaging. Radiol Clin North Am 1992; 30:777–787.
9. Hricak H, Finck S, Honda G, Göranson H. MR imaging in the evaluation of benign uterine masses: value of gadopentetate dimeglumine–enhanced T1-weighted images. AJR 1992; 158:1043–1053.
10. Upadhyaya NB, Doody M, Googe PB. Histopathologic changes in leiomyoma treated with leuprolide acetate. Fertil Steril 1990; 54:811–814.
11. Uemura T, Mori J, Yoshimura Y, Minaguchi H. Treatment effects of GnRH agonist on the binding of estrogen and progesterone, and the histological findings of uterine leiomyomas. Asia-Oceania J Obstet Gynecol 1991; 17:315–320.